Basis functions for the consistent and accurate representation of surface mass loading

Peter J. Clarke[1,*], David A. Lavallée[1], Geoff Blewitt[1,2], Tonie van Dam[3]

[1] School of Civil Engineering and Geosciences, Cassie Building, Newcastle University, Newcastle NE1 7RU, UK.

[2] Mackay School of Earth Science and Engineering, Mail Stop 178, University of Nevada, Reno, NV 89557-0088, USA.

[3] Faculty of Sciences, Technology and Communication, University of Luxembourg, 6 rue Richard Coudenhove-Kalergi, L-1359, Luxembourg.

Submitted to *Geophysical Journal International*.

Accepted ____________. Received ____________, in original form 23 January 2007.

Short title: BASIS FUNCTIONS FOR SURFACE MASS LOADING

[*] corresponding author: tel. +44 (0)191 222 6351, fax +44 (0)191 222 6502, e-mail Peter.Clarke@newcastle.ac.uk.

This is an electronic version of an article published in Geophys. J. Int., 171(1), 1-10 (doi:10.1111/j.1365-246X.2007.03493.x).

Summary

Inversion of geodetic site displacement data to infer surface mass loads has previously been demonstrated using a spherical harmonic representation of the load. This method suffers from the continent-rich, ocean-poor distribution of the geodetic data, coupled with the predominance of the continental load (water storage and atmospheric pressure) compared with the ocean bottom pressure (including the inverse barometer response). Finer-scale inversion becomes unstable due to the rapidly increasing number of parameters which are poorly constrained by the data geometry. Several approaches have previously been tried to mitigate this, including the adoption of constraints over the oceanic domain derived from ocean circulation models, the use of smoothness constraints for the oceanic load, and the incorporation of GRACE gravity field data. However, these methods do not provide appropriate treatment of mass conservation and of the ocean's equilibrium-tide response to the total gravitational field. Instead, we propose a modified set of basis functions as an alternative to standard spherical harmonics. Our basis functions allow variability of the load over continental regions, but impose global mass conservation and equilibrium tidal behaviour of the oceans.

We test our basis functions first for the efficiency of fitting to realistic modelled surface loads, and then for accuracy of the estimates of the inferred load compared with the known model load, using synthetic geodetic displacements with real GPS network geometry. Compared to standard spherical harmonics, our basis functions yield a better fit to the model loads over the period 1997-2005, for an equivalent number of parameters, and provide a more accurate and stable fit using the synthetic geodetic displacements. In particular, recovery of the low-degree coefficients is greatly improved. Using a 9-parameter fit we are able to model 58% of the variance in the synthetic degree-1 zonal coefficient time series, 38-41% of the degree-1 non-zonal coefficients, and 80% of the degree-2 zonal coefficient. An equivalent spherical harmonic estimate truncated at degree 2 is able to model the degree-1 zonal coefficient similarly (56% of variance), but only models 59% of the degree-2 zonal coefficient variance and is unable to model the degree-1 non-zonal coefficients.

Keywords: Geodesy, Spherical harmonics, Numerical techniques, Global Positioning System (GPS), Surface mass loading, Water cycle, Geocenter,.

1. Introduction

Forward modelling of geodetic site displacements due to surface mass loading is frequently performed using gridded surface mass datasets and a Green's function approach (*e.g.* Farrell, 1972), but because these Green’s functions are reference frame dependent, it may be difficult to account properly for the effects of geocenter motion (Blewitt, 2003). Spherical harmonic representation allows the transparent use of the correct reference frame dependent Love numbers and so does not suffer from this drawback in forward modelling, but fine-scale (higher-degree) inversion of surface mass loads from geodetic displacements becomes unstable due to the continent-rich, ocean-poor distribution of the geodetic data (Wu *et al*., 2002). A further problem, which affects both the Green’s function and spherical harmonic methods, but is more readily correctable using the spherical harmonic approach, is the appropriate treatment of mass conservation and of the ocean’s equilibrium-tide response to the total gravitational field (Dahlen, 1976; Wahr, 1982; Mitrovica *et al.*, 1994; Blewitt & Clarke, 2003; Clarke *et al.*, 2005). The primary aim of this paper is to show how a modified set of basis functions derived from mass-conserving, tidally-equilibrated, land area-masked spherical harmonics can be used to overcome some of these limitations.

Our target is the robust estimation of surface mass loading at weekly and longer timescales. Figure 1 shows the spatial variation of the root mean square (rms) weekly change in total surface mass load predicted by some recent models over the period 1997–2005. The total load comprises three components. Firstly, it includes land hydrology, here taken from the LaD model (Milly & Shmakin, 2002), which assimilates selected river discharge data into a global model of water and energy balance. Secondly, it incorporates ECCO ocean bottom pressure data (http://www.ecco-group.org) which results from the assimilation of wind stress, heat flux, and freshwater flux observations into a global ocean circulation model. Thirdly, it includes atmospheric pressure data from the NCEP reanalysis (Kalnay *et al.*, 1996); this is set to zero over the oceans, and we apply the mass conservation procedure of Clarke *et al.* (2005) which effectively provides the required inverse barometer correction. It is readily apparent that the variability in the continental load is far greater than that over the oceans.

If standard spherical harmonics are used as basis functions to describe this surface mass load (or the corresponding surface displacements), a high truncation degree is required to represent the coastline in sufficient detail and maintain a smooth, small oceanic load. Conversely, when inverting geodetic surface displacement data to estimate the load, little information is available over the oceans, so the solution becomes biased and unstable even at low degrees unless *a priori* oceanic constraints are applied (Wu *et al.*, 2003, 2006; Kusche & Schrama, 2005). Moreover, the actual variability in oceanic load is predominantly that due to ocean – land mass transfer and the ocean's equilibrium tidal response to the land load, not that due to other changes in the ocean (Clarke *et al.*, 2005).

We therefore desire an alternative means of representing the surface mass load, that is consistent with the physics of the ocean's response to the total load, and is adapted to but not unduly constrained by the expected characteristics of the load. In other words, the basis functions must allow considerable spatial variability over land but preserve a smooth oceanic domain, whilst conserving mass globally. In this paper, we present and test a modified spherical harmonic basis that achieves this goal. In some respects, the method is analogous to the use of spherical cap harmonics or Slepian functions (*e.g.* Thébault *et al.*, 2004; Simons & Dahlen, 2006) in that it is a data-driven approach with minimal physical model assumptions, but the approach is here adapted to the specific physical problem of the spatial distribution of oceans and continents.

2. Forming the basis functions

We adopt the spherical harmonic convention used by Blewitt & Clarke (2003) but with 4π-normalisation applied. Briefly, we use classical, real-valued spherical harmonics with the phase convention of Lambeck (1988). Expressing all loads in terms of the equivalent height of a column of seawater, density ρ_S, the total time-variable load T may be expressed as a function of geographic position Ω (latitude ϕ, longitude λ) as

$$T(\Omega) = \sum_{n=1}^{\infty} \sum_{m=0}^{n} \sum_{\Phi}^{\{C,S\}} T_{nm}^{\Phi} Y_{nm}^{\Phi}(\Omega) \tag{1}$$

Summation begins at $n = 1$ because conservation of mass requires that T_{00} should vanish, although as discussed by Blewitt & Clarke (2003) a degree-zero term could be included to absorb any measurement scale error. The resulting change in potential at the reference surface (the initial geoid), due to the effect of the load itself and the accompanying deformation of the Earth, is (Farrell, 1972)

$$V(\Omega)=\tfrac{3g\rho_S}{\rho_E}\sum_{n=1}^{\infty}\sum_{m=0}^{n}\sum_{\Phi}^{\{C,S\}}\tfrac{1+k_n'}{2n+1}T_{nm}^{\Phi}Y_{nm}^{\Phi}(\Omega) \qquad (2)$$

where ρ_E is the mean density of the solid Earth, g is the acceleration due to gravity at its surface, and k_n' is the static gravitational load Love number for degree n. The surface of the solid Earth will change in height by

$$H(\Omega)=\tfrac{3\rho_S}{\rho_E}\sum_{n=1}^{\infty}\sum_{m=0}^{n}\sum_{\Phi}^{\{C,S\}}\tfrac{h_n'}{2n+1}T_{nm}^{\Phi}Y_{nm}^{\Phi}(\Omega) \qquad (3)$$

and will be displaced eastwards and northwards by

$$E(\Omega)=\tfrac{3\rho_S}{\rho_E}\sum_{n=1}^{\infty}\sum_{m=0}^{n}\sum_{\Phi}^{\{C,S\}}\tfrac{l_n'}{2n+1}T_{nm}^{\Phi}\frac{\partial_\lambda Y_{nm}^{\Phi}(\Omega)}{\cos\varphi}$$

$$N(\Omega)=\tfrac{3\rho_S}{\rho_E}\sum_{n=1}^{\infty}\sum_{m=0}^{n}\sum_{\Phi}^{\{C,S\}}\tfrac{l_n'}{2n+1}T_{nm}^{\Phi}\partial_\varphi Y_{nm}^{\Phi}(\Omega) \qquad (4)$$

where h_n' and l_n' are the height and lateral load Love numbers respectively. The degree-1 Love numbers h_1' and l_1' are specific to the chosen reference frame (Blewitt, 2003). In this paper, we use Love numbers derived (D. Han, personal communication) using the spherically-symmetric, non-rotating, elastic, isotropic PREM Earth model (Dziewonski and Anderson, 1981) and expressed in the reference frame of the centre of mass (CM) of the whole Earth system (Blewitt, 2003).

Rather than using standard spherical harmonic functions $Y_{nm}^{\Phi}(\Omega)$, we form initial basis functions $B_{nm}'^{\Phi}(\Omega)$ by masking each $Y_{nm}^{\Phi}(\Omega)$ using an ocean function $C(\Omega)$, defined to be zero in land areas and unity over the oceans:

$$\begin{aligned}B_{nm}'^{\Phi}(\Omega)&=\{1-C(\Omega)\}\cdot Y_{nm}^{\Phi}(\Omega)\\&\approx\sum_{n'=0}^{N'}\sum_{m'=0}^{n'}\sum_{\Phi'}^{\{C,S\}}a_{nm,n'm'}'^{\Phi,\Phi'}Y_{n'm'}^{\Phi'}(\Omega)\end{aligned} \qquad (5)$$

The coefficients $a_{nm,n'm'}'^{\Phi,\Phi'}$ can be derived from the spherical harmonic expansion of $C(\Omega)$, to arbitrary degree and order, using Clebsch-Gordan coefficients for multiplication in the spectral domain (Blewitt *et al.*, 2005), although in our case (5) is truncated at degree N'. In this paper, we set N' to 30, which allows our basis functions to represent the coastline of all major land masses acceptably. Note that the summation in (5) begins at $n' = 0$, not $n' = 1$, because each $B'^{\Phi}_{nm}(\Omega)$ may involve a gain or loss of mass from the land area which, after masking, will no longer be balanced by mass changes in the oceanic domain. We then correct these raw $B'^{\Phi}_{nm}(\Omega)$, which are non-zero on land only, by adding an oceanic term $S(\Omega)$. This term represents the "sea-level equation" (Dahlen, 1976) which enforces global mass conservation and allows the ocean to respond gravitationally to the land load:

$$\begin{aligned} B^{\Phi}_{nm}(\Omega) &= B'^{\Phi}_{nm}(\Omega) + S^{\Phi}_{nm}(\Omega) \\ S^{\Phi}_{nm}(\Omega) &= C(\Omega) \cdot \{(V(\Omega) + \Delta V)/g - H(\Omega)\} \end{aligned} \qquad (6)$$

where the spatially-varying terms $H(\Omega)$ and $V(\Omega)$ are the Earth response to a total load $B^{\Phi}_{nm}(\Omega)$ as defined in (2) and (3), and the spatially-constant term ΔV accounts for global conservation of mass. The coefficients of $B'^{\Phi}_{nm}(\Omega)$ and $B^{\Phi}_{nm}(\Omega)$ implicitly have the same units as $T(\Omega)$, *i.e.* height of an equivalent column of sea water. Equations (2, 3, 6) are solved by the method of Clarke *et al.* (2005). Here, we take initial spherical harmonics $Y^{\Phi}_{nm}(\Omega)$ from degree zero to degree and order 10, truncating the ocean function at degree 40, and our final $B^{\Phi}_{nm}(\Omega)$ at degree 30. Because of selection rules governing the nonzero products of two associated Legendre polynomials (see Appendix B of Blewitt and Clarke, 2003), the latter truncation is the maximum degree that is always exactly computed for our truncation of $Y^{\Phi}_{nm}(\Omega)$ and $C(\Omega)$.

We now have corrected basis functions $B^{\Phi}_{nm}(\Omega)$ defined by their truncated spherical harmonic expansions:

$$B^{\Phi}_{nm}(\Omega) = \sum_{n'=1}^{N'} \sum_{m'=0}^{n'} \sum_{\Phi'}^{\{C,S\}} a^{\Phi,\Phi'}_{nm,n'm'} Y^{\Phi'}_{n'm'}(\Omega) \qquad (7)$$

noting that this summation begins from $n' = 1$ because these functions are mass-conserving. It might be argued that compared with standard spherical harmonics, these basis functions are less able to represent general surface mass loads, because following (5) and (6) the only signal that can be represented in oceanic regions is the mass-conserving equilibrium tidal response. However, we reiterate that dynamic ocean loads are small compared with loads over the continents (Figure 1). We will show in Section 3 that the new basis functions are capable of better overall representation of typical surface loads, for a given number of coefficients, and in Sections 4 and 5 that they permit a more stable and globally accurate inversion from realistic geodetic data.

Although it is not strictly necessary, we normalise the coefficients $a_{nm,n'm'}^{\Phi,\Phi'}$ such that

$$\iint B_{nm}^{\Phi}(\Omega) B_{nm}^{\Phi}(\Omega) \cos\varphi \, d\varphi \, d\lambda = 1 \qquad (8).$$

However, the $B_{nm}^{\Phi}(\Omega)$ are not orthonormal; in general

$$\iint B_{nm}^{\Phi}(\Omega) B_{n'm'}^{\Phi'}(\Omega) \cos\varphi \, d\varphi \, d\lambda \neq 0 \qquad (9)$$

unlike the analogous spherical harmonic functions. Figure 2 shows the departure from orthogonality. This is generally small, but some prominent differences are seen, arising from the strong global asymmetry of continent-ocean distribution. Because our basis functions are not orthogonal, we must estimate them to data by least squares rather than global convolution. In practice, this is not the disadvantage compared with standard spherical harmonics that it might first appear, because convolution can in any case only be applied to global datasets and not to the discrete site displacements that are obtained from a real geodetic network.

In the following sections, we will assess the utility of our basis functions by comparing the goodness of fit of a set of $\overline{N}(\overline{N}+2)$ coefficients T_{nm}^{Φ} for standard spherical harmonic functions, truncated at degree $\overline{N}$, to a synthetic dataset based on a known load $\overline{T}(\Omega)$

$$\overline{T}(\Omega) \approx T(\Omega) = \sum_{n=1}^{\overline{N}} \sum_{m=0}^{n} \sum_{\Phi}^{\{C,S\}} T_{nm}^{\Phi} Y_{nm}^{\Phi}(\Omega) \qquad (10)$$

with the goodness of fit of a set of $(N+1)^2$ coefficients $\hat{T}_{nm}^{\Phi}$ for our new basis functions corresponding to spherical harmonics up to degree N, to the same synthetic dataset

$$\overline{T}(\Omega) \approx \hat{T}(\Omega) = \sum_{n=0}^{N} \sum_{m=0}^{n} \sum_{\Phi'}^{\{C,S\}} \hat{T}_{nm}^{\Phi} B_{nm}^{\Phi}(\Omega) \qquad (11).$$

After estimation, we may compare the goodness of fit in the spatial domain, or perform a coefficient-by-coefficient comparison by transforming the $\hat{T}_{nm}^{\Phi}$ into coefficients $\tilde{T}_{nm}^{\Phi}$ of standard spherical harmonics using (7) and (11):

$$\begin{aligned}\hat{T}(\Omega) &= \sum_{n=0}^{N}\sum_{m=0}^{n}\sum_{\Phi'}^{\{C,S\}} \hat{T}_{nm}^{\Phi} B_{nm}^{\Phi}(\Omega) \\ &= \sum_{n=0}^{N}\sum_{m=0}^{n}\sum_{\Phi}^{\{C,S\}} \hat{T}_{nm}^{\Phi} \left\{ \sum_{n'=1}^{N'}\sum_{m'=0}^{n'}\sum_{\Phi'}^{\{C,S\}} a_{nm,n'm'}^{\Phi,\Phi'} Y_{n'm'}^{\Phi'}(\Omega) \right\} \\ &= \sum_{n'=1}^{N'}\sum_{m'=0}^{n'}\sum_{\Phi'}^{\{C,S\}} \left\{ \sum_{n=0}^{N}\sum_{m=0}^{n}\sum_{\Phi}^{\{C,S\}} a_{nm,n'm'}^{\Phi,\Phi'} \hat{T}_{nm}^{\Phi} \right\} Y_{n'm'}^{\Phi'}(\Omega) \\ &= \sum_{n'=1}^{N'}\sum_{m'=0}^{n'}\sum_{\Phi'}^{\{C,S\}} \tilde{T}_{n'm'}^{\Phi'} Y_{n'm'}^{\Phi'}(\Omega)\end{aligned} \qquad (12)$$

where

$$\tilde{T}_{n'm'}^{\Phi'} = \sum_{n=0}^{N}\sum_{m=0}^{n}\sum_{\Phi}^{\{C,S\}} a_{nm,n'm'}^{\Phi,\Phi'} \hat{T}_{nm}^{\Phi} \qquad (13).$$

Note again that in (12) the upper degree limit N' refers to the level of detail to which the basis functions are themselves represented in (7). This is not related to the number of estimated coefficients in (11), which depends on N; in general, $N' >> N$.

3. Efficiency of fit to synthetic load data

The efficiency of a set of basis functions may be expressed as the number of coefficients that is required to explain a certain proportion of the variance in a dataset. We test the efficiency of our basis functions by fitting them to the synthetic load dataset described above, evaluated at weekly intervals spanning GPS weeks 0898 – 1322 (mid-week dates 23 Mar 1997 – 08 May 2005). The atmospheric and oceanic components of the load are obtained by weekly averaging of the 6-hourly NCEP and ECCO data respectively. The continental water storage component is linearly interpolated from the monthly outputs of the LaD model. Each component of the load is represented using spherical harmonics up to degree 100. The total load is first corrected to enforce conservation of mass and the tidal oceanic response, and then evaluated at points on a global 2°×2° grid.

As Figure 3 shows, our basis functions consistently require fewer coefficients to model a given fraction of the variance in the synthetic dataset, compared with the equivalent spherical harmonic basis set. The saving in number of parameters to achieve the same goodness of fit is typically a factor of 2–3, *i.e.* the new basis functions are as good a spherical harmonic fit truncated one or two degrees higher. We conclude that our basis functions are well suited to the description of realistic surface mass loads, even though they impose no *a priori* information of the behaviour of the dominating continental hydrological and atmospheric components of the load, nor of dynamic ocean circulation effects.

4. Global accuracy of fit to synthetic loading displacements

The inverse problem faced by geodesists differs from the above in two respects. Firstly, the global surface displacement field is attenuated at higher degrees, compared with the load, and this worsens the estimation of the higher-degree load coefficients. More importantly, real geodetic displacement data do not sample the planet evenly, and the sampling is biased towards continental regions (for GPS data, particularly western Europe and North America). Goodness of fit at the sample locations does not necessarily imply global fidelity of the estimated load to the true signal. Because we are here using a synthetic dataset, we can test the accuracy of our fit by comparing the known load with that generated from our estimated coefficients, over the entire Earth's surface. This will allow us to compare the sampling bias that occurs when using our basis functions with the bias that occurs when using standard spherical harmonics.

We test accuracy of fit by using the synthetic surface mass load time series described above to generate weekly 3-D displacements at sites in the International GNSS Service (IGS) network, from which we estimate the surface mass load. The geometry and spatial sampling density of the IGS network have changed significantly since its inception in the early 1990s, but the weekly solutions obtained by individual Analysis Centres (ACs) do not necessarily reflect these changes directly. For example, ACs may choose to maintain a more or less even global distribution of sites at the expense of the total number of sites processed, or they may prefer to focus on a particular region. To illustrate these network-specific effects, we perform our weekly estimations using site distributions from two AC networks typifying these differing strategies (Figure 4). The NASA Jet Propulsion Laboratory (JPL) AC solutions contain a slowly increasing number of sites, from ~40 in 1997 to ~75 in 2005, but the inter-hemispheric site distribution remains roughly constant, with ~50%, ~60% and ~60% of sites in the hemispheres centred on the positive X, Y and

Z axes respectively (a perfectly even network would have 50% of its sites in each hemisphere). In contrast, the Scripps Institution of Oceanography (SIO) reanalysis AC solutions enlarge dramatically over the same period from ~90 stations in early 1997 to ~130 from late 1998 onwards, with roughly constant inter-hemispheric bias at a higher level that that of the JPL AC (~40%, ~60% and ~75% of sites in the positive X, Y and Z hemispheres).

At each weekly epoch, the site coordinates in the AC solution (or their residuals to the long-term trend) will contain correlated random errors with stochastic properties that should be reflected in the variance-covariance matrix (VCM). The magnitude of the coordinate variances and the structure of the VCMs will change with time, depending on a number of factors including not only GPS network distribution and data volume but also advances in the models applied in GPS analysis software. We incorporate these factors into our investigation by adding random noise to each synthetic weekly dataset, with a VCM derived from the appropriate weekly AC solution. The JPL and SIO ACs should both adhere to the same IERS standards (McCarthy, 1996; McCarthy & Petit, 2004) in their analysis, but JPL and SIO use different processing strategies and software (GIPSY/OASIS II and GAMIT/GLOBK respectively). We account for issues of absolute VCM scaling that arise from this, by re-scaling each weekly VCM so that the variance of unit weight after estimating linear site velocities is unity. Because this solution does not include loading parameters, the re-scaling will result in a slightly conservative but nonetheless realistic estimate of the VCM. However, the estimated load will only depend on inter-site correlations and the relative weighting of sites within a weekly AC solution; the absolute scaling of the VCM is of secondary importance.

Systematic errors caused by spatial and temporal correlations in real GPS data that are not properly modelled in the AC processing will not be reflected in the VCM, and these may affect the estimation of loading parameters from real data. Based on the comparison of geocenter motion estimates from GPS data, SLR data, and surface mass load models Lavallée *et al.* (2006) suggest that the effects of such systematic errors on low-degree coefficients of the surface mass load are small. In any case, systematic errors will have little effect on our assessment of the relative performance of different basis function sets.

We estimate a set of $\bar{N}(\bar{N}+2)$ coefficients for standard spherical harmonic functions, truncated at degree $\bar{N}$, to each weekly synthetic dataset according to (10). Similarly, we estimate $(N+1)^2$ coefficients for our new basis functions derived from spherical harmonics up to degree N, to the same synthetic datasets. Henceforth we refer to both $\bar{N}$ and N as the maximum degree of fit, because these quantities relate to the number of estimated parameters, although the new basis functions are expanded to the much higher degree N' ($N'=30$ in this paper).

The goodness of fit between the synthetic and estimated surface mass loads can be considered in a variety of ways. Figure 5 shows the rms true (synthetic) degree amplitudes compared with the rms estimated degree amplitude and rms misfit degree amplitude for both sets of basis functions, computed over the entire time series. The degree amplitudes A_n are defined for the set of coefficients T_{nm}^{Φ} by:

$$A_n^2 = \sum_{m=0}^{n} \sum_{\Phi}^{\{C,S\}} \left(T_{nm}^{\Phi}\right)^2 \qquad (14)$$

and similarly for $\tilde{A}_n$ in terms of $\tilde{T}_{nm}^{\Phi}$. The misfit degree amplitudes Ξ_n^2 with respect to the coefficients $\bar{T}_{nm}^{\Phi}$ of the known load are given by:

$$\Xi_n^2 = \sum_{m=0}^{n} \sum_{\Phi}^{\{C,S\}} \left(T_{nm}^{\Phi} - \bar{T}_{nm}^{\Phi}\right)^2 \qquad (15).$$

We see that the spherical harmonic basis leads to higher misfit levels and tends to overestimate the degree amplitude, whereas using the new basis results in degree amplitudes close to the synthetic "truth", and lower misfit levels suggesting a favourable signal/noise ratio. For standard spherical harmonics, the effect is stronger for the more asymmetric SIO network geometry than for the more balanced JPL network geometry (Figure 5). In contrast, the new basis functions are much less sensitive to network geometry, showing little difference between the JPL and SIO networks in terms of estimated and misfit degree amplitudes. Over the whole time series, use of basis functions derived from degrees up to 4 yields the best comparison with the true degree amplitudes up to degree 10. For the earlier JPL networks (weeks 900-999), a maximum degree of 3 or 4 is optimal, whereas for the later epochs (weeks 1200-1299) the maximum degree could reasonably be increased to 5 or even 6 (Figure 6). Similar time dependency is found for the SIO network, although the level of misfit is generally higher. Hereafter we discuss results based on the JPL network geometry only.

We also consider the spatial distribution of the root mean square difference between synthetic and estimated loads at each point on the Earth's surface (Figure 7). At maximum fitted degree 4, the new basis functions are able to represent much of the signal over Eurasia and northern America, although this is at the expense of poorer accuracy over equatorial Africa and America, where there are fewer GPS sites. In contrast, the standard spherical harmonic basis functions lead to higher rms differences over the entire ocean and are unable to fit the data as well. For maximum degree 6, this is even more pronounced: although the new basis functions show localised instability in Africa, America and Antarctica, standard spherical harmonics show instability that is even more geographically widespread.

5. Accuracy of estimated low-degree load coefficients

GPS observations can add the most to our knowledge of the surface mass loading at low degrees (Kusche & Schrama, 2005), because GRACE recovery of the gravity field is least sensitive at these long wavelengths. The utility of GPS estimates of loading may therefore lie in the accuracy of low-degree coefficients rather than the spatial detail of the estimated load. Figure 8 and Table 1 compare the "true" (synthetic) and estimated coefficients for degree 1. For the degree-1 coefficients, the new basis functions give a consistently better fit to the "true" loading, for an equivalent number of estimated parameters. For T_{11}^{C}, standard spherical harmonics seem particularly unable to fit the data; this presumably results from a combination of network geometry and aliasing, with the vast majority of continents and hence GPS sites being situated in the hemisphere centred on the positive X axis. The new basis functions are significantly less affected by this problem. T_{11}^{C} is slightly less extreme, but again the new basis functions are consistently better throughout the time series and this advantage becomes more pronounced during the latter half. T_{10}^{C} is estimated slightly better by spherical harmonics in the case of degree-1 truncation, but at all higher truncation degrees the new basis functions outperform standard spherical harmonics.

Both sets of basis functions are able to fit the low-degree zonal coefficients T_{20}^C and T_{30}^C reasonably accurately (Figure 9, Table 1), although the new basis is slightly better in each case because it is less prone to "overshoot" at the seasonal extreme values. For T_{40}^C, the new basis functions are considerably more accurate at fitting the synthetic data; this feature persists throughout the time series and demonstrates the ability of the new basis functions to track moderate-degree features of the surface mass load even with relatively sparse data geometry. A maximum degree of 3 or 4 (16 or 25 estimated parameters) gives the best overall fit to the low-degree coefficients, over the whole time series.

For comparison with previous published results which have tended to concentrate on the seasonal fit to the data, we also compare the seasonal periodic (annual and semi-annual harmonic) variation in the estimated low-degree coefficients (Table 2, Table 3). We see that the annual and semi-annual harmonic fit to T_{10}^C is reasonably robust, regardless of the basis set and the maximum degree of fit. The annual fit to T_{11}^C is very poor for standard spherical harmonics, although the fit to the small semi-annual signal is fortuitously good. For T_{11}^S, the annual spherical harmonic fit is reasonably accurate in amplitude but almost in quadrature to the "true" signal; again the semi-annual signal is small. For all of these coefficients and for T_{20}^C, the new basis functions are well able to track both the annual and semi-annual signals.

6. Discussion and conclusions

We have demonstrated that a physically reasonable set of basis functions, derived from spherical harmonics, can be used to represent the variation in surface mass load and associated displacements of the solid Earth. Our representation achieves better fit to realistic synthetic data than does a spherical harmonic estimate with the same degree of freedom, is more robust to the biasing effect of network geometry, and is less prone to widespread oscillation in unconstrained regions. Our results represent a lower bound on the uncertainty with which the low-degree surface mass loads can be estimated using GPS. Non-equilibrium ocean loads are not presently included in our method, but they are small compared with the land load. If GPS network geometry were favourable, it would be possible to include a complementary set of mass-conserving basis functions, zeroed on land, to model the dynamic ocean load at low degrees. The truncation level of this complementary basis set could be chosen independently to that of the land-oriented basis set, to allow for the lower density of oceanic GPS sites. Systematic errors not accounted for in the formal variance-covariance matrix of GPS solutions will add further biases to the estimates, but these should reduce in future as the GPS measurement model improves.

The basis functions directly incorporate the physics of reference frame definition, conservation of mass, and equilibrium ocean response to the land load, whilst parameterising the land load in a way that is independent of any hydrological or climate model. Previous inversion schemes (Wu *et al.*, 2003, 2006; Kusche & Schrama, 2005) have incorporated information from models or other satellite data, either directly or via an oceanic smoothing constraint. Our method allows the use of GPS data alone to estimate the low-degree coefficients of the surface mass load. GRACE data are unable to recover the degree-1 load coefficients, and at degrees 2 – 4, GPS data are expected to contribute the majority of the data strength in a combined GPS – GRACE inversion (Kusche & Schrama, 2005). GPS data have to date only been demonstrated to recover the seasonal and interannual variations in the surface mass load, not the secular variations, because of the difficulty of isolating the effects of the latter from plate tectonic and post-glacial rebound motions. However, we expect future improvements in the modelling of glacio-isostatic adjustment to enable the use of GPS to estimate secular changes in surface mass loading.

References

Blewitt, G. (2003). Self-consistency in reference frames, geocenter definition, and surface loading of the solid Earth. *J. Geophys. Res.*, **108**(B2), 2103.

Blewitt, G., & P. Clarke (2003). Inversion of Earth's changing shape to weigh sea level in static equilibrium with surface mass redistribution. *J. Geophys. Res.*, **108**(B6), 2311.

Blewitt, G., D. Lavallée, P. Clarke & K. Nurutdinov (2005). Application of Clebsch-Gordan coefficients and isomorphic frame transformations to invert Earth's changing geometrical shape for continental hydrological loading and sea level's passive response. In *A Window on the Future of Geodesy [Proc. IAG General Assembly, Sapporo, Japan, 2003]*, International Association of Geodesy Symposia, **128**, 518-523.

Clarke, P.J., D.A. Lavallée, G. Blewitt, T. van Dam & J.M. Wahr (2005). Effect of gravitational consistency and mass conservation on seasonal surface loading models. *Geophys. Res. Lett.*, **32**(8), L08306.

Dahlen, F. A. (1976). The passive influence of the oceans upon the rotation of the Earth. *Geophys. J. R. Astr. Soc.*, **46,** 363–406.

Dziewonski, A. D. & D. L. Anderson (1981). Preliminary Reference Earth Model. *Phys. Earth planet. Inter.*, **25,** 297–356.

Farrell, W.E. (1972). Deformation of the Earth by surface loads. *Rev. Geophys.* **10**, 761-797.

Kalnay, E., *et al.* (1996). The NCEP/NCAR 40-year reanalysis project. *Bull. Am. Meteorol. Soc.* **77**(3), 437-471.

Kusche, J. & E.J.O. Schrama (2005). Surface mass redistribution inversion from global GPS deformation and Gravity Recovery and Climate Experiment (GRACE) gravity data. *J. Geophys. Res.*, **110**, B09409 (doi:10.1029/2004JB003556).

Lambeck, K. (1988). *Geophysical geodesy*. Oxford: Oxford University Press.

Lavallée, D.A., T. van Dam, G. Blewitt & P.J. Clarke (2006). Geocenter motions from GPS: a unified observation model. *J. Geophys. Res.*, **111**(B5), B05405 (doi:10.1029/2005JB003784).

McCarthy, D.D. (1996). *IERS conventions (1996)*. IERS Technical Note 21, Frankfurt: BKG.

McCarthy, D.D. & G. Petit (2004). *IERS conventions (2003)*. IERS Technical Note 32, Frankfurt: BKG.

Milly, P.C.D. & A.B. Shmakin (2002). Global modeling of land water and energy balances: Part 1. The Land Dynamics (LaD) Model. *J. Hydrometeorology,* **3**(3), 283–299.

Mitrovica, J.X., J.L. Davis & I.I. Shapiro (1994). A spectral formalism for computing three-dimensional deformations due to surface loads: 1. Theory. *J. Geophys. Res.*, **99**, 7057–7073.

Simons, F.J. & F.A. Dahlen (2006). Spherical Slepian functions and the polar gap in geodesy. *Geophys. J. Int.* **166**, 1039–1061.

Thébault, E., J.J. Schott, M. Mandea & J.P. Hoffbeck (2004). A new proposal for spherical cap harmonic modelling. *Geophys. J. Int.* **159**, 83–103.

Wahr, J. (1982). The effects of the atmosphere and oceans on the Earth's wobble – I. Theory. *Geophys. J. R. Astr. Soc.*, **70**, 349-372.

Wu, X., D.F. Argus, M.B. Heflin, E.R. Ivins & F.H. Webb (2002). Site distribution and aliasing effects in the inversion for load coefficients and geocenter motion from GPS data. *Geophys. Res. Lett.*, **29**(24), 2210.

Wu, X., M.B. Heflin, E.R. Ivins, D.F. Argus & F.H. Webb (2003). Large-scale global surface mass variations inferred from GPS measurements of load-induced deformation. *Geophys. Res. Lett.*, **30**(14), 1742.

Wu, X., M.B. Heflin, E.R. Ivins & I. Fukumori (2006). Seasonal and interannual global surface mass variations from multisatellite geodetic data. *J. Geophys. Res.*, **111**, B09401.

Acknowledgements

This work was funded in the UK by Natural Environment Research Council grant NER/A/S/2001/01166 to PJC and a Royal Society University Research Fellowship to DAL, and in the USA by NASA and NSF grants to GB. We would like to thank the authors of the LaD, NCEP and ECCO datasets for making their results widely available. The Consortium for Estimating the Circulation and Climate of the Ocean (ECCO) is funded by the US National Oceanographic Partnership program. Constructive comments by Xiaoping (Frank) Wu and an anonymous reviewer did much to improve our original manuscript.

Table 1. Root mean square goodness of fit between synthetic and estimated low-degree load coefficients, for varying maximum degrees of estimation. Units are mm of sea-water equivalent. Top figure is rms residual to estimate using new basis functions; lower figure is rms residual to estimate using standard spherical harmonics. Numbers in parentheses represent model skill (the fitted percentage of variance in that coefficient); an asterisk denotes negative skill (the residual variance is greater than that of the original synthetic coefficient).

	Signal rms	**Max deg 1**	**Max deg 2**	**Max deg 3**	**Max deg 4**
T_{10}^{C}	9.16	8.14 (21%) 7.09 (40%)	5.92 (58%) 6.05 (56%)	5.94 (58%) 5.65 (62%)	5.35 (66%) 5.85 (59%)
T_{11}^{C}	6.29	5.06 (35%) 6.23 (2%)	4.95 (38%) 6.42 (*)	4.69 (44%) 6.37 (*)	4.81 (42%) 6.65 (*)
T_{11}^{S}	5.98	4.42 (45%) 6.50 (*)	4.60 (41%) 6.12 (*)	4.50 (43%) 6.40 (*)	4.44 (45%) 6.28 (*)
T_{20}^{C}	11.34		5.07 (80%) 7.26 (59%)	4.82 (82%) 5.74 (74%)	5.07 (80%) 6.30 (69%)
T_{30}^{C}	10.80			5.14 (77%) 5.66 (73%)	4.74 (81%) 5.52 (74%)
T_{40}^{C}	6.92				4.56 (57%) 6.07 (23%)

Table 2. Annual harmonic terms fitted to the estimated low-degree load coefficients, for varying maximum degrees of estimate, compared with those fitted to the synthetic dataset. Units of amplitude are mm of sea-water equivalent; phases are in degrees. The upper figure is obtained using the new basis functions; the lower figure is obtained using standard spherical harmonics.

Coeff	**Synthetic**		**Max deg 1**		**Max deg 2**		**Max deg 3**		**Max deg 4**	
	amp	**pha**	**amp**	**pha**	**amp**	**pha**	**amp**	**pha**	**amp**	**pha**
T_{10}^{C}	9.42	58	16.40	48	11.60	47	12.25	52	10.77	53
			13.50	48	8.62	43	9.94	54	7.14	52
T_{11}^{C}	6.91	25	8.55	33	6.69	32	6.42	43	5.61	41
			0.96	75	0.43	98	0.75	95	0.48	162
T_{11}^{S}	7.01	-24	6.13	-23	5.36	-38	5.05	-40	5.08	-36
			4.95	49	3.45	46	3.51	53	2.90	53
T_{20}^{C}	13.09	62			14.48	69	11.29	63	12.33	62
					17.64	79	14.87	69	16.92	69
T_{30}^{C}	12.88	132					12.94	126	11.92	133
							15.31	137	14.72	135
T_{40}^{C}	4.53	120							4.66	111
									2.31	178

Table 3. As Table 2, but for semi-annual harmonic terms.

Coeff	Synthetic amp	Synthetic pha	Max deg 1 amp	Max deg 1 pha	Max deg 2 amp	Max deg 2 pha	Max deg 3 amp	Max deg 3 pha	Max deg 4 amp	Max deg 4 pha
T_{10}^{C}	3.94	-150	3.96	-161	4.08	-175	3.82	-174	3.74	-166
			2.62	-150	1.88	-166	2.41	-160	1.67	-154
T_{11}^{C}	0.33	165	0.18	-35	0.39	-54	0.36	-67	0.65	-89
			0.29	-51	0.17	-34	0.21	-52	0.12	-29
T_{11}^{S}	0.97	178	1.35	-168	1.12	-177	1.25	-178	1.32	-175
			1.35	-143	1.03	-151	1.17	-155	0.79	-135
T_{20}^{C}	2.81	-72			2.49	-84	2.30	-75	2.19	-77
					3.25	-99	2.57	-83	2.58	-88
T_{30}^{C}	2.82	-159					2.76	-156	3.14	-162
							2.68	-142	4.00	-166
T_{40}^{C}	4.31	-21							4.56	-31
									6.36	-25

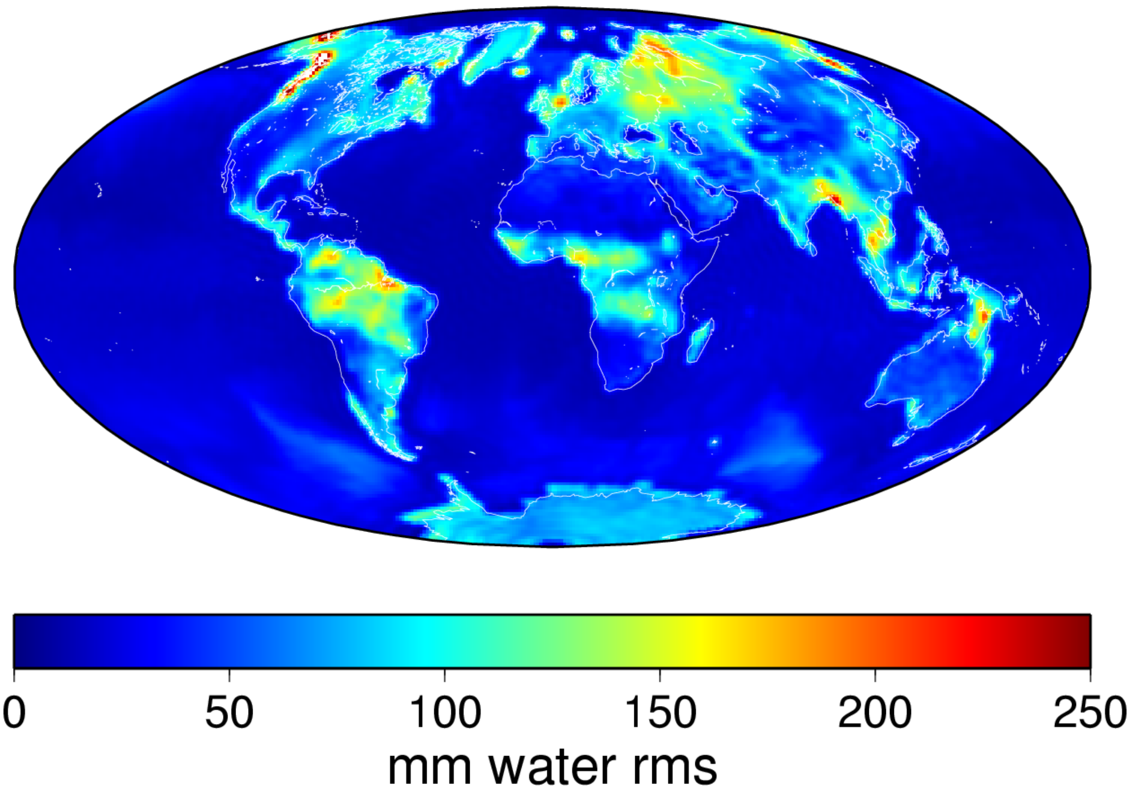

Figure 1. Root mean square weekly variability in surface mass load over the period 1997–2005 (expressed as the height of an equivalent column of seawater), predicted by the combination of the LaD (continental hydrology), NCEP Reanalysis (atmospheric pressure), and ECCO (ocean bottom pressure) models, corrected for overall mass conservation.

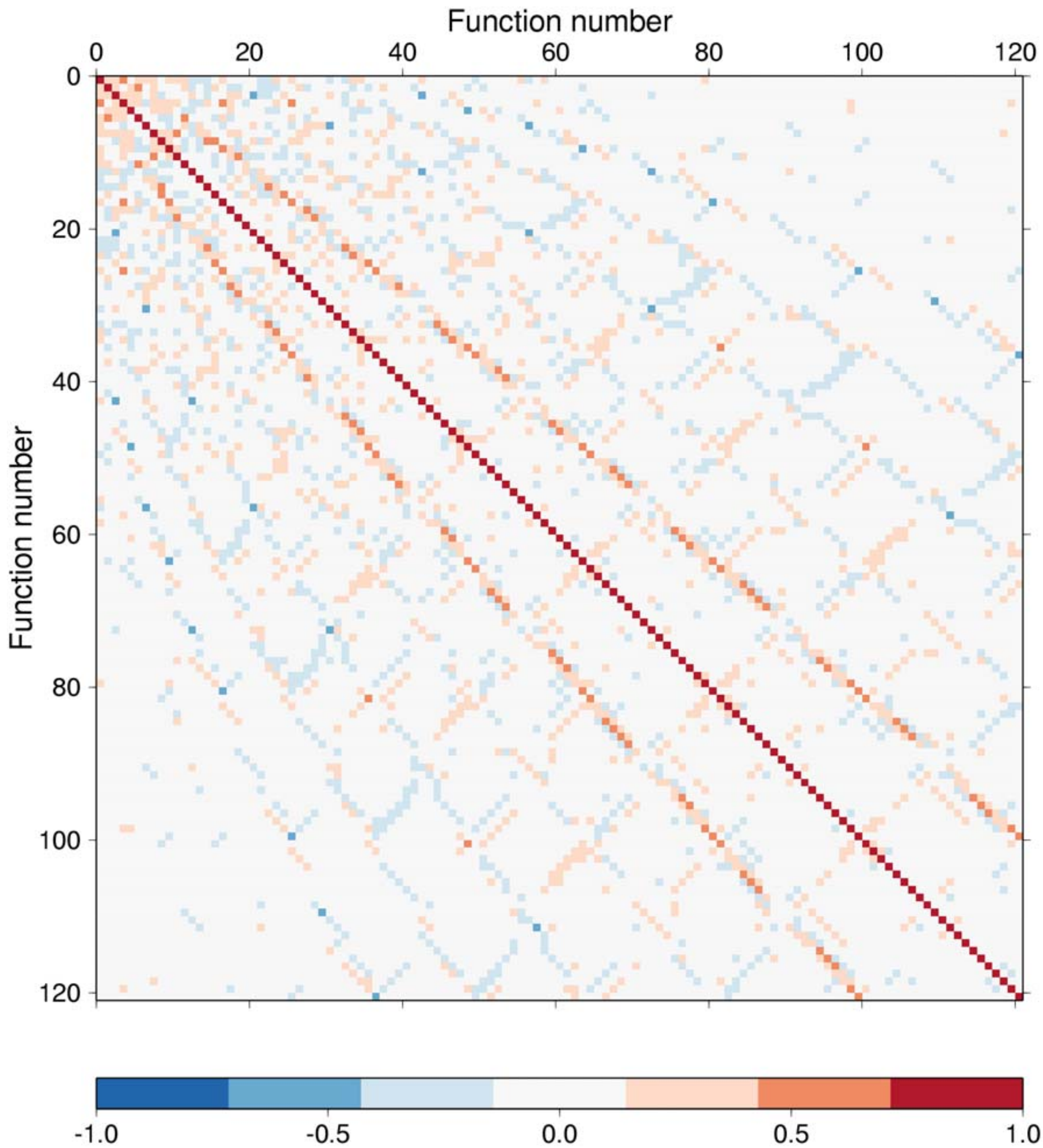

Figure 2. Departure from orthogonality of the normalised basis functions $B_{nm}^{\Phi}(\Omega)$. The function number is given by $n(n+1)+m$ for $\Phi = C$, and $n(n+1)-m$ for $\Phi = S$.

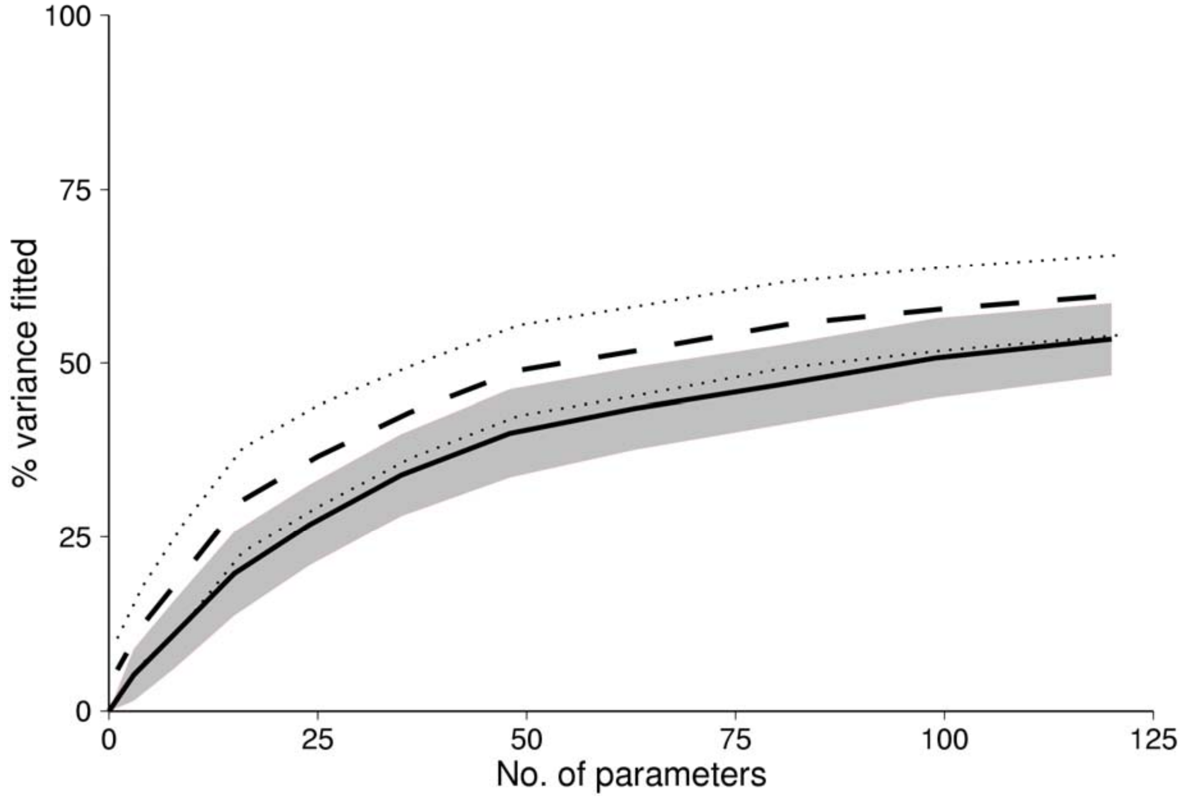

Figure 3. Mean and standard deviation, over the period 1997–2005, of the percentage of load variance fitted by standard spherical harmonics (solid line and shaded area) and by the new basis functions (dashed line and dotted bounds), as a function of the number of estimated parameters at each epoch.

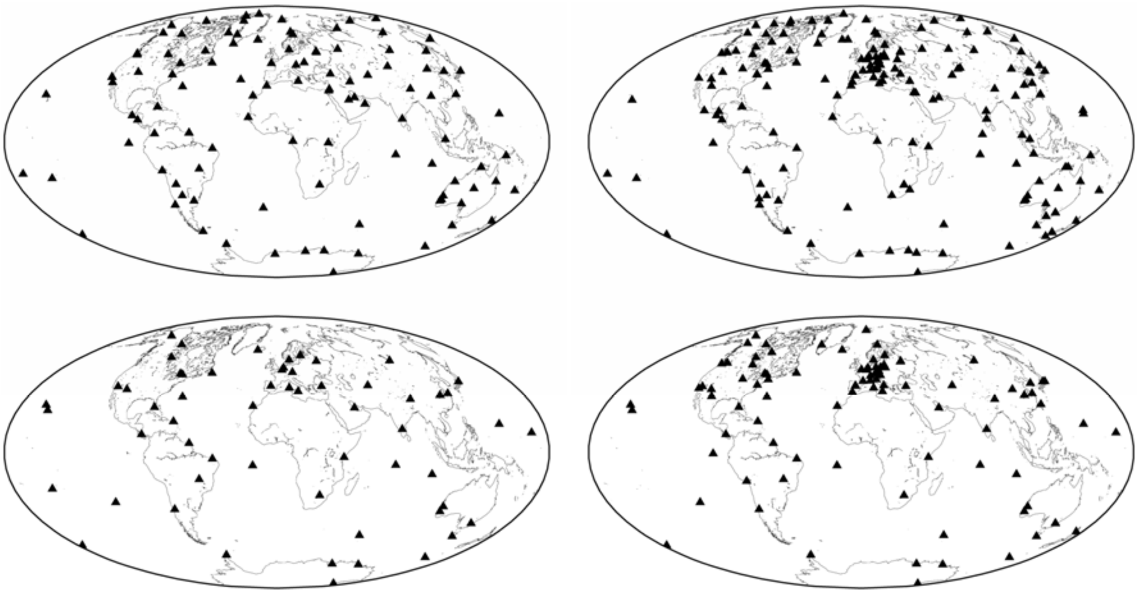

Figure 4. The JPL (left) and SIO-reanalysis (right) AC networks for GPS weeks 0898 (top) and 1322 (bottom).

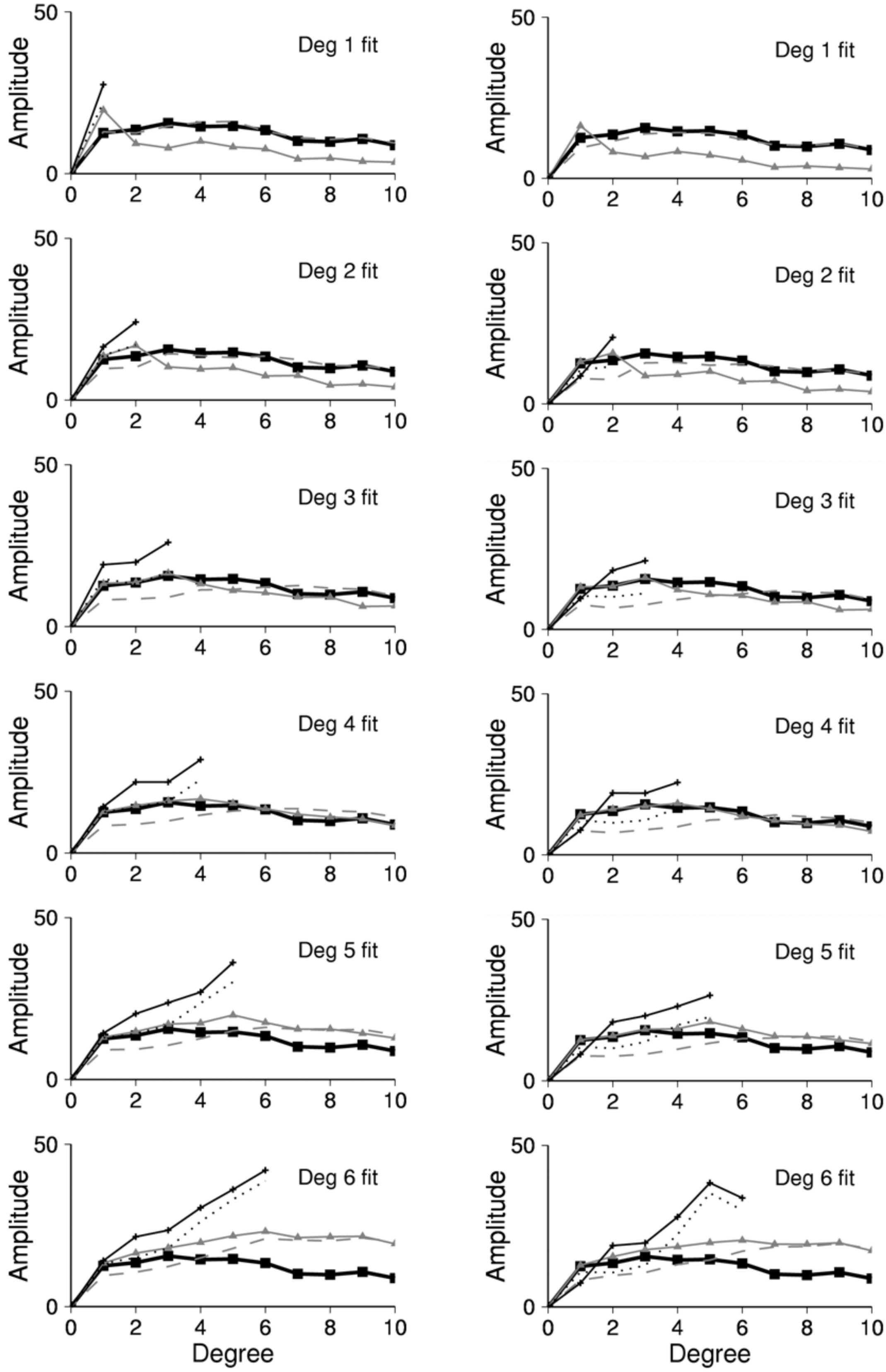

Figure 5. Root mean square degree amplitude of the estimated load (solid lines) and misfit degree amplitude (pecked lines) using standard spherical harmonic basis functions

(black/dotted lines with crosses), and the new basis functions (grey/dashed lines and triangles), computed over the entire time series for various maximum degrees of fit. The true (synthetic) degree amplitude is shown as a heavy line in each plot. Amplitude units are mm of seawater equivalent to the surface load. (left) SIO network, (right) JPL network.

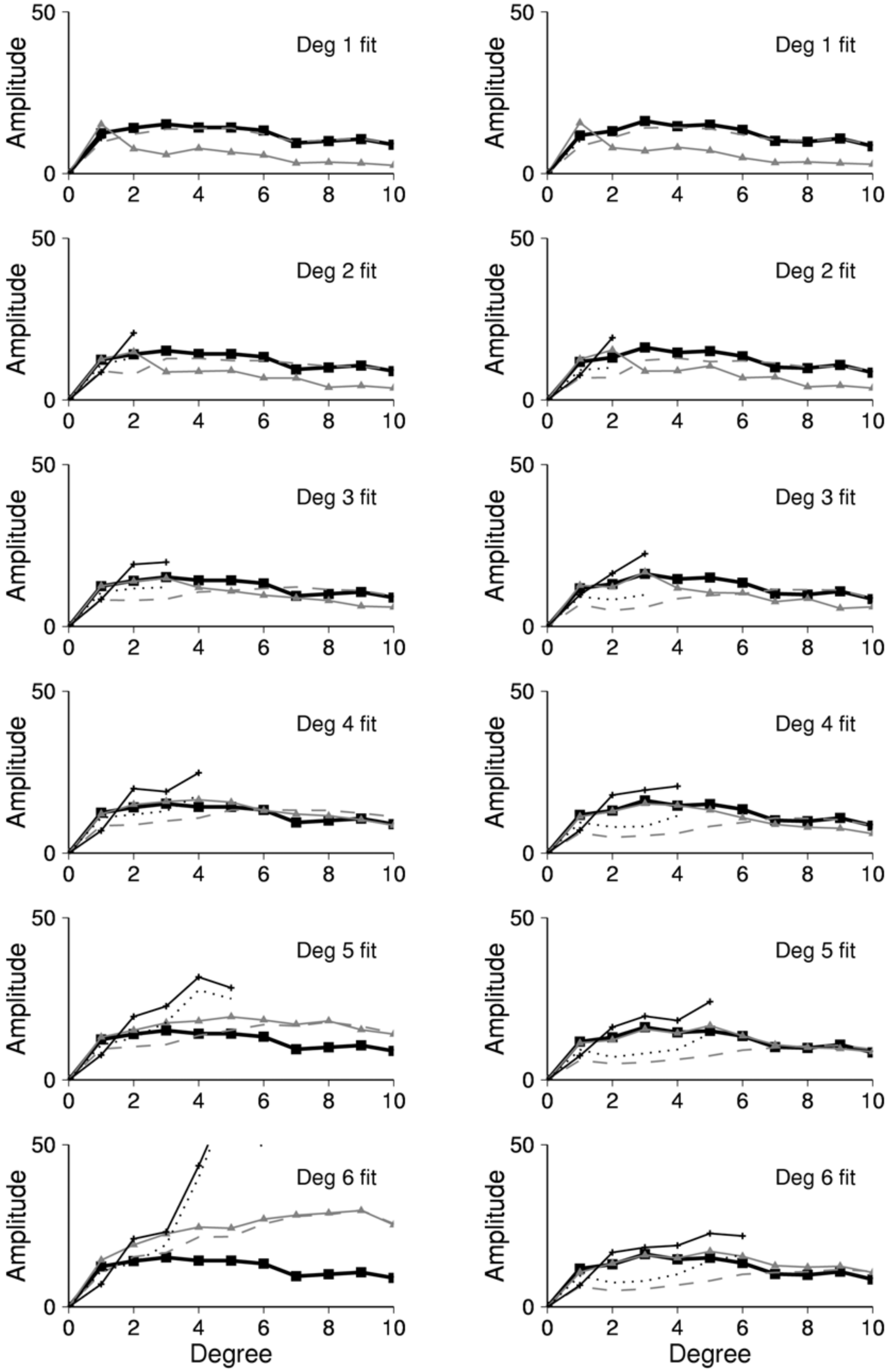

Figure 6. As Figure 5, but for the JPL network geometry with estimated and misfit degree amplitudes computed over weeks 900–999 (left) and weeks 1200–1299 (right).

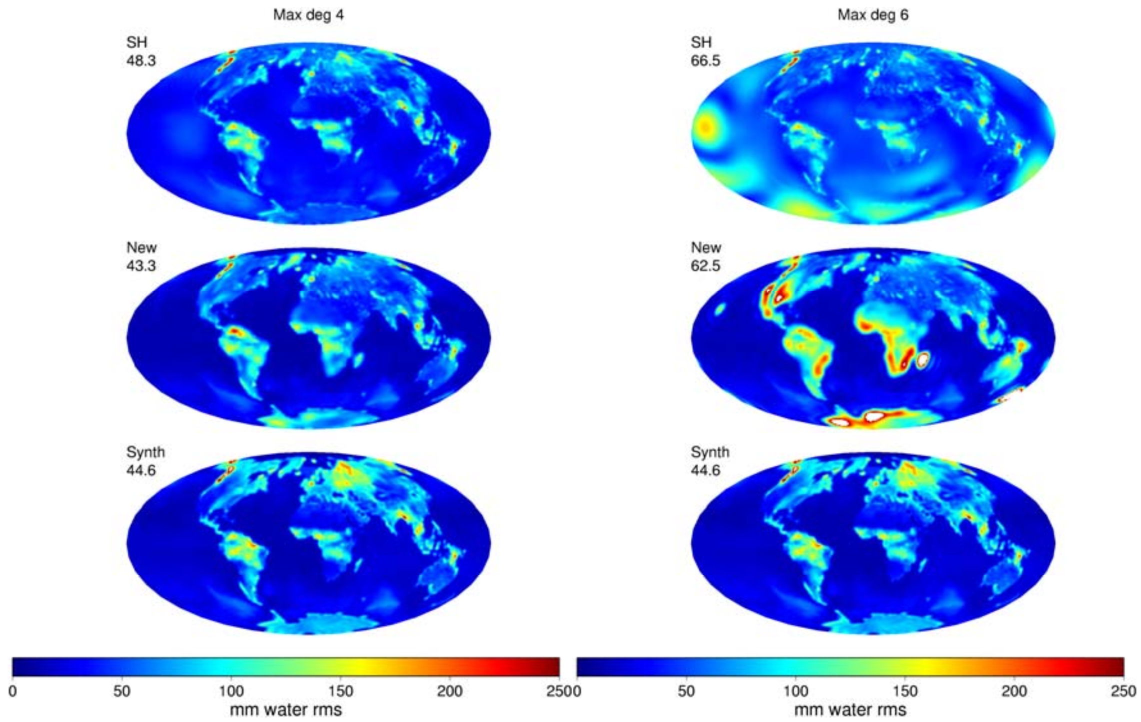

Figure 7. Spatial distribution of root mean square misfit between estimated surface loads and synthetic data, computed over the entire time series, for estimates truncated at degree 4 (left) and 6 (right). The bottom plots show the variability of the synthetic data. Numbers indicate the overall root mean square of the misfit/data (in mm). The inversion data have JPL network geometry.

(a)

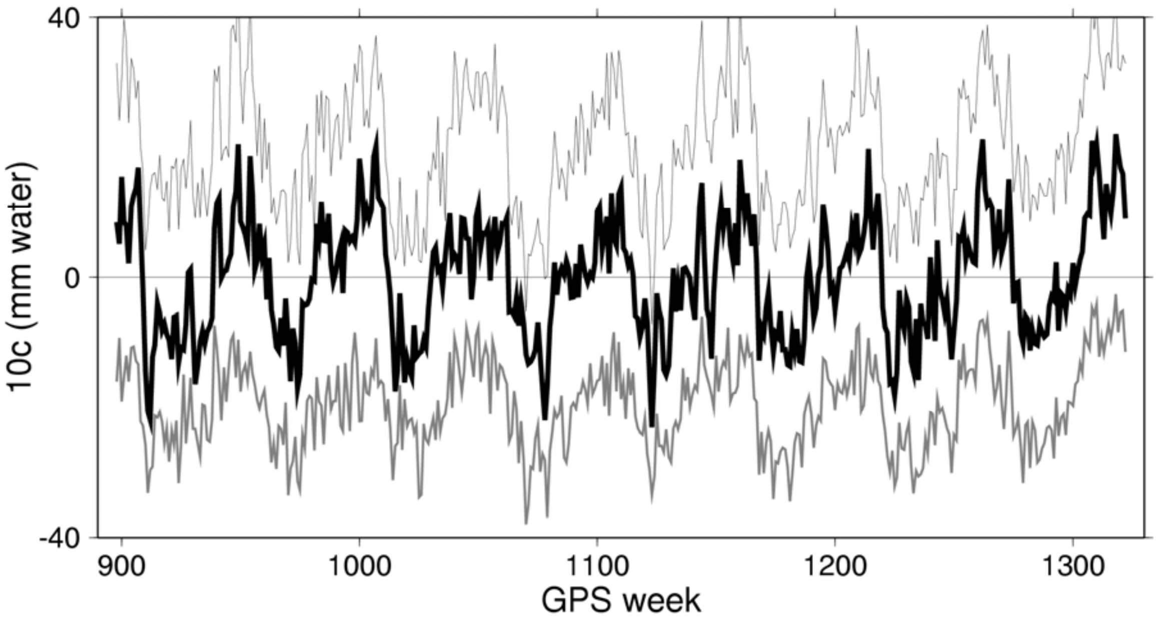
40
0
-40
10c (mm water)
900
1000
1100
1200
1300
GPS week

(b)

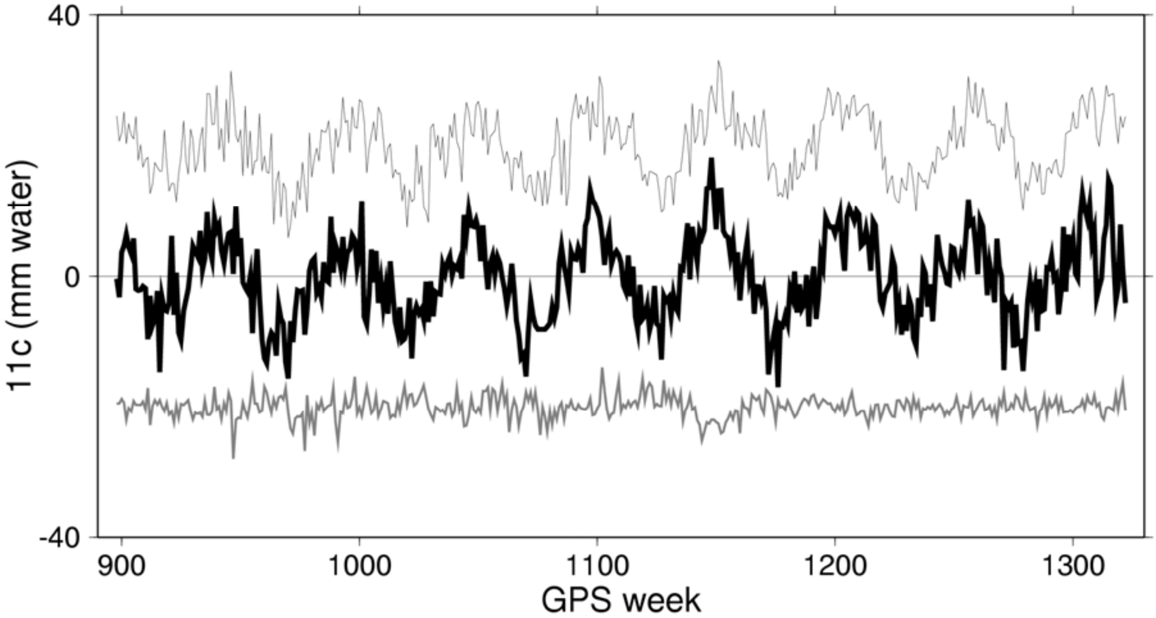
40
0
-40
11c (mm water)
900
1000
1100
1200
1300
GPS week

(c)

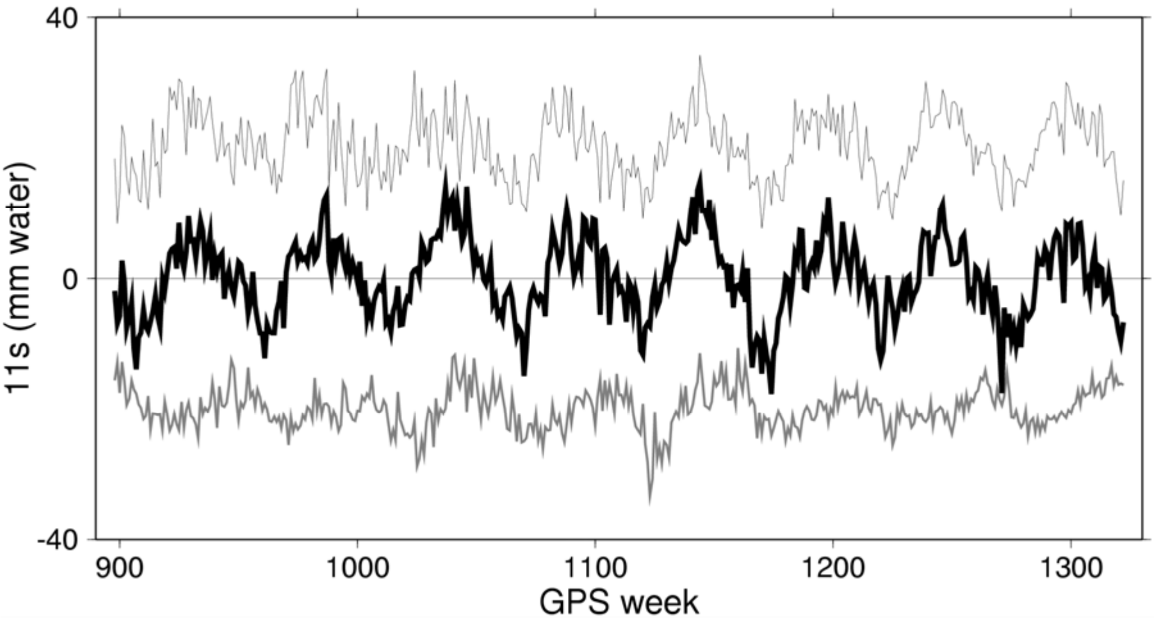

Figure 8. **(a)** Comparison between synthetic load coefficient T_{10}^{C} (heavy line) and its estimate using standard spherical harmonic basis functions (grey line, offset by -10) and the new basis functions (thin line, offset by +10). JPL network geometry is used, with maximum degree of fit 4. Amplitude units are mm of seawater equivalent to the surface load.

(b, c) As Figure 8(a) but for coefficient T_{11}^{C} **(b)**, T_{11}^{S} **(c)**.

(a)

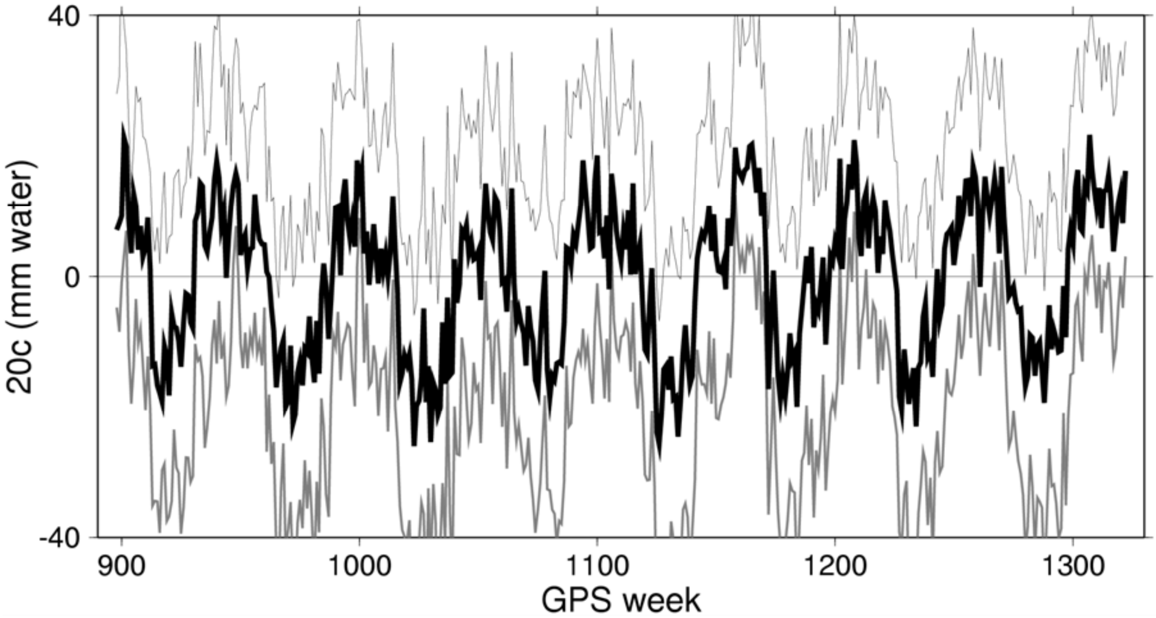
40
0
-40
20c (mm water)
900
1000
1100
1200
1300
GPS week

(b)

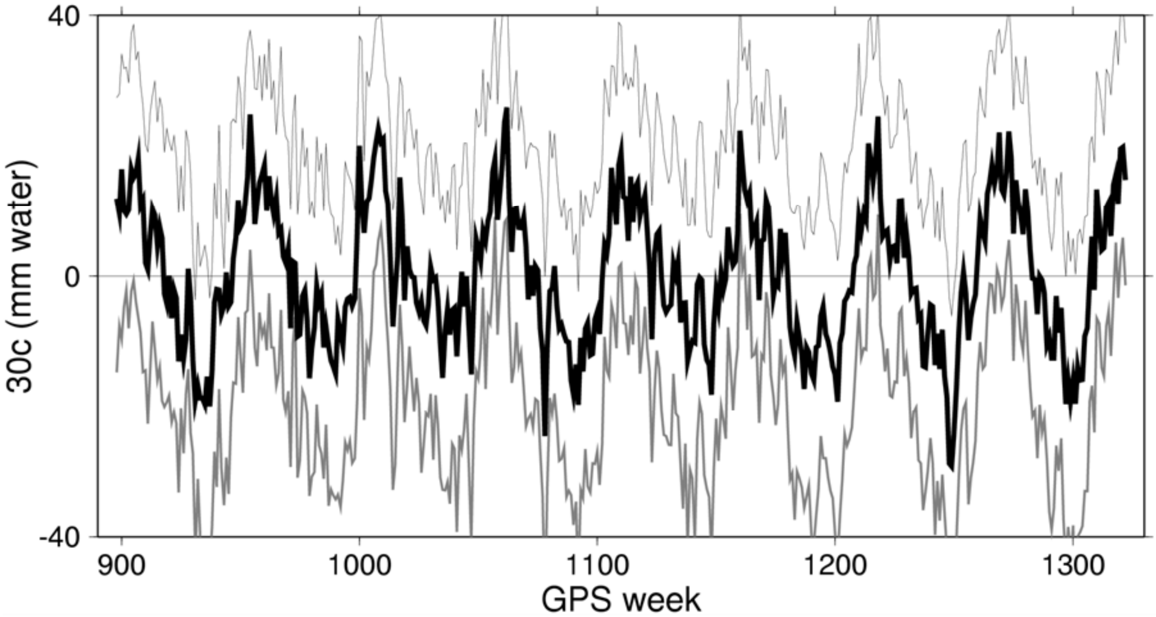
40
0
-40
30c (mm water)
900
1000
1100
1200
1300
GPS week

582 **(c)**

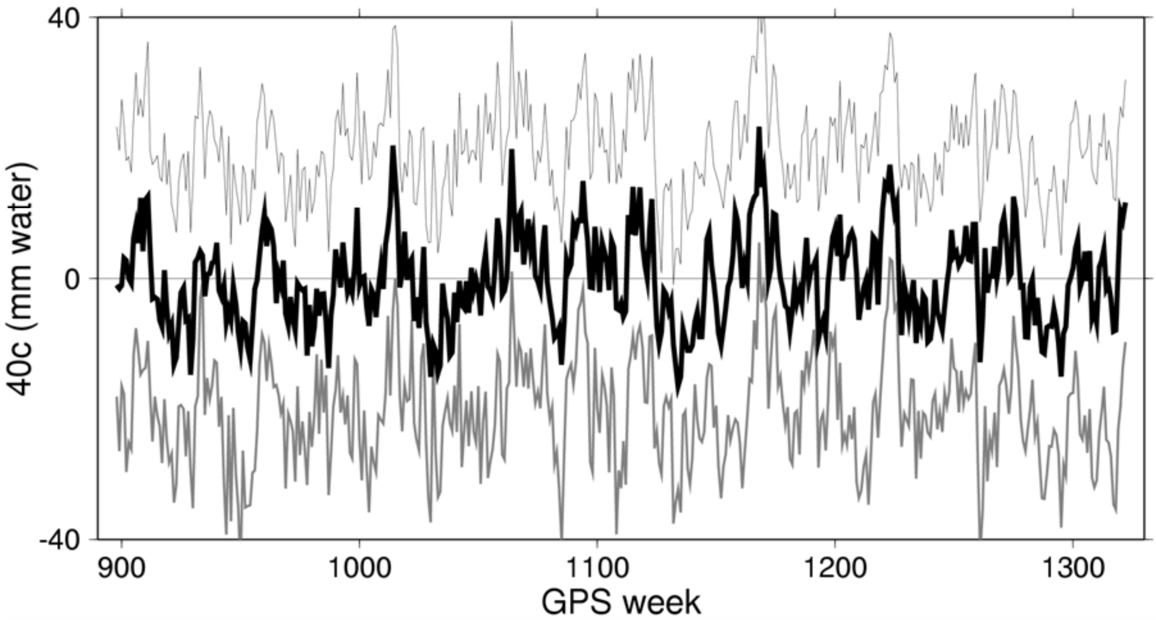

583

584

585 **Figure 9.** As Figure 8 but for coefficients T_{20}^{C} **(a)**, T_{30}^{C} **(b)**, T_{40}^{C} **(c)**.